

Characterisation of PVD Lumogen® films for wavelength conversion applications

Alec Deslandes^a, A. Bruce Wedding^b, Stephen R. Clarke^a,
Janis G. Matisons^a and Jamie S. Quinton^{*a}

^a School of Chemistry, Physics & Earth Sciences, Flinders University, Adelaide, Australia

^b School of Electrical & Information Engineering, University of South Australia, Adelaide, Australia

ABSTRACT

Lumogen Yellow S0790 is a commercial azomethine based pigment and is used for enhancing CCD devices for detecting ultraviolet radiation. In this work we report on the crystal structure and morphology of the raw material, as-deposited and post-annealed films, as well as the influence these have on the subsequent optical properties. Our measurements of physical vapour deposited (PVD) Lumogen films indicate that commercial Lumogen powder is crystalline in its as-received state, with a melting point of 273.3°C and boiling point of 328.6°C. Furthermore, we have found that as-deposited films on room temperature substrates possess an inherent crystalline structure, which has not been reported previously, but also that the material's structure changes into a completely different crystalline form upon annealing for 90 hours at 80°C.

Keywords: PVD, Lumogen, Up-shifter, CCD detectors, Thin films, Crystallinity

1. INTRODUCTION

The ability to alter a given material's surface properties in order to improve its suitability in a given environment or alter its aesthetic appeal, thus enabling it for a new technological application, is one of the chief aims of surface science. In particular, fluorescent dyes are frequently often employed as surface coatings, or even incorporated into the matrix of a material, to alter its photonic properties. One such dye, Lumogen® Yellow S 0790, is used for a variety of applications, ranging from being a marker in crop dusting, crack detection and as a pigment for crayons and paints. The chemical structure of Lumogen, or 2-hydroxy-[(2-hydroxy-1-naphthalenyl)methylene]hydrazone, which comprises an hydroxyl terminated naphthalene group attached to each end of an azomethine chain, is shown in figure 1.

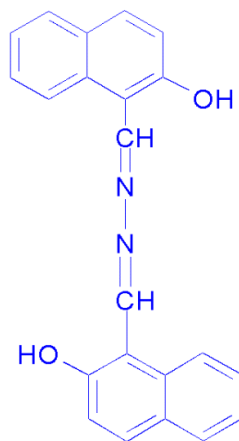


Figure 1. The chemical structure of Lumogen Yellow S0790.

* Corresponding Author. Email: Jamie.Quinton@flinders.edu.au

One of the more high-technological applications for Lumogen Yellow lies in its use as a wavelength up-shifter, whereby short wavelength ultraviolet (UV) light that is absorbed by the material is rapidly re-emitted with longer wavelengths in the visible spectrum, for improving the spectral response of charge-coupled device (CCD) detectors. Such detectors, which have low noise, a large dynamic range, linearity, a high quantum efficiency (QE) in the visible and x-ray regions [1] but experience an enhanced UV response when coated with a thin Lumogen film.

Employment of a thin, translucent Lumogen film on the front side of the CCD enhances the UV response of the device, but a small penalty is paid in the visible region due to attenuation by the overlayer film. One method of overcoming this is to make the silicon substrate thin (10-40 μm thick) and illuminate the coating from the rear side [2]. This method bypasses the problem of the gate structures on the front of the CCD, and can lead to an average quantum efficiency of more than 40% for wavelengths in the range of 116 to 400 nm.

While Lumogen Yellow S0790 is not the only choice of wavelength up-shifting material that is available or could be employed to improve device QE in the UV region, previous studies by Kristianpoller and others have shown that Lumogen is superior to coronene and sodium salicylate dye materials as the latter have less-uniform spectral response in the UV region than Lumogen does (with Dutton[3] and Knapp[4]). For example, coronene has a local minimum in the spectral response curve at approximately 380nm and silicon CCDs experience a UV response cut-off at around 400nm [5], thus a coronene coated CCD exhibits a bandpass type behaviour where UV light in between those limits (ie from ~380-400nm) would be relatively undetected. Lumogen, however, does not exhibit any non-uniformity in the spectral response and is thus a superior candidate for UV conversion and detection.

It is this enhanced quantum efficiency in the UV region that makes Lumogen of paramount importance in current UV-imaging technologies, and it has been employed in high-end astronomical systems by NASA/JPL (Jet Propulsion Laboratory), for example, on the Hubble Space Telescope and the Cassini-Huygens spacecraft. It is only with the direct assistance of a Lumogen coating on the imaging CCD array that Cassini has very recently been able to show the existence of ice on Phoebe, a natural satellite in the Saturnian system.

Notwithstanding the superior optical properties of Lumogen for UV detection applications, Kristianpoller and Dutton noticed that a clear and transparent evaporated film would turn cloudy after a few days or weeks of storage at room temperature, and attributed this change to partial crystallisation within the film [3]. They also reported that the luminescence efficiency of these films does not change despite a suggested phase transition. Further reports of crystallisation within these films were reported in a NASA/JPL report, in which a number of Lumogen coated CCDs failed quality control specifications due to visible variations across the film and between samples prepared under identical conditions [6]. In that report, visible variation across the film was attributed to patches of crystal growth. It was found that this non-uniform growth led to pixel-to-pixel imaging nonuniformity across the CCD.

More recently, Janesick reported results of scanning electron Microscopy (SEM) studies into crystallisation within Lumogen films[7]. Films that were deposited onto room temperature substrates were found to have an increase in QE as crystals formed naturally over time. Images were also published showing films deposited onto substrates at elevated temperature, showing that the as-deposited film possessed a homogeneous structure, before developing large crystals after a high temperature bake.

The lack of understanding in the extent of crystallinity and its influence on the properties and performance of devices that contain these coatings provides the underlying motivation for our ongoing work in this area. It is possible that crystalline Lumogen films may have advantageous optical qualities and characteristics that could be harnessed to improve the coating and hence CCD performance. The ability to control the growth of crystals within these films and to do so uniformly would lead to each coated CCD pixel in an array having identical saturation levels. Therefore, the length of exposure/incoming signal that each pixel on the CCD can handle before becoming saturated would be optimised.

2. EXPERIMENTAL

In addition to measurements of the as-received Lumogen powder, physical vapour deposition (PVD) was employed to deposit the Lumogen coatings on flat glass substrates. PVD was achieved in a scratch-built vacuum system at the University of South Australia, which is based on heating a crucible containing the raw coating material, as illustrated in a schematic diagram of the instrument depicted in figure 2.

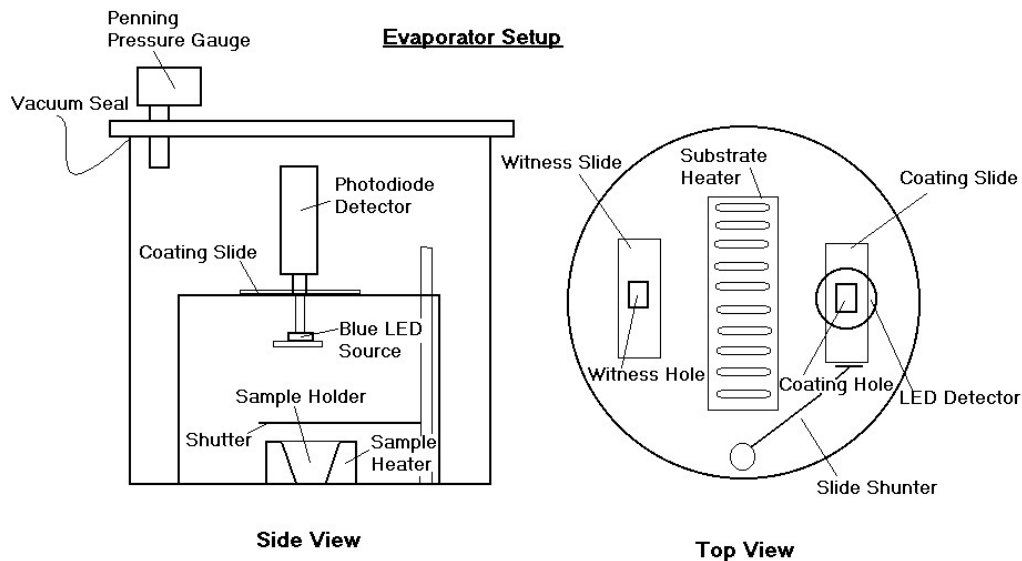


Figure 2. Schematic of the PVD system used to deposit Lumogen films

The system is pumped by a rotary vane type backing and an oil diffusion pump, with a base pressure better than 10^{-6} Torr. As can be seen in the figure, the sample to be evaporated onto the substrate is placed in the crucible oven and heated to its sublimation point. The top view of the apparatus shows the three types of slides that are produced during a coating process. Typically, four glass slides (in a 2x2 arrangement) form the samples of interest and are placed under the substrate heater, which may be used to control the substrate temperature if desired during deposition. In addition to these, a witness slide, which is a room temperature substrate for comparison and a coating slide, which uses an optical detection arrangement of a blue LED and a photodiode detector to optically monitor the thickness of the deposited film, are used for diagnostic purposes.

The procedure for coating glass slides with Lumogen largely follows that employed by JPL [8]. Glass substrate slides were cleaned with acetone, ethanol and methanol before positioning in the deposition system. After the methanol wash, the solvent was evaporated with a hot air stream, before being placed in the vacuum system for coating. For coating deposition, the sample oven was first filled with Lumogen Yellow S 0790, a powder in its as received state (99.9% pure, supplied by BASF). After the system reached medium vacuum, the crucible oven was switched on and the temperature monitored via a copper-constantan thermocouple. The voltage applied to the heater was typically such that the measured temperature increased at approximately 8°C per minute up to the desired deposition temperature of 270°C . The shutter was then opened to allow sublimated Lumogen to deposit onto the under-side of the substrates.

For studying the coating properties, the samples were characterised at the University of South Australia using the Ian Wark Research Institute's scanning electron microscope (SEM) facility; and at Flinders with differential scanning calorimetry (DSC), using a 2920 MDSC V2.6A instrument, thermogravimetric analysis (TGA) using an AutoTGA 2950HR V6.1A instrument, UV-visible absorption spectrophotometry a Cary model 50 instrument, X-ray Diffraction (XRD) using a Phillips X-ray Diffractometer that has a Cobalt $K_{\alpha,1}$ source of characteristic wavelength 1.789\AA .

3. RESULTS

3.1 Thermophysical Properties of Lumogen

Lumogen Yellow S0790 is a powder in its as-received state. Our initial investigations involved probing the thermophysical properties of the material to understand its behaviour in the oven prior to deposition. These investigations were made with thermogravimetric analysis (TGA) and scanning differential calorimetry (DSC).

The TGA technique involves heating a small mass of the substance in air and measuring changes in mass as a function of temperature. The TGA thermogram obtained for Lumogen powder is presented in figure 3.

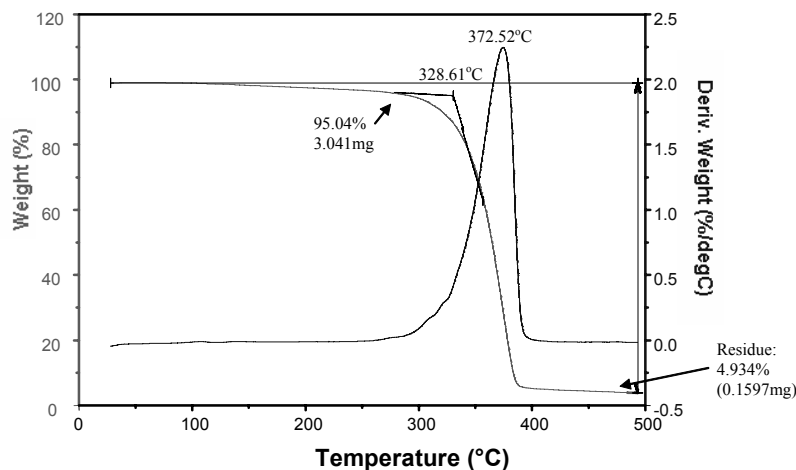


Figure 3. TGA thermogram of Lumogen powder. The figure illustrates two curves versus temperature. The monotonically decreasing curve is Weight(%) (plotted against the left hand ordinate axis scale) of Lumogen versus temperature; the second containing the peak is the derivative of Weight(%) (plotted against the right hand ordinate axis scale).

In the figure, the mass of the material (expressed as % weight, plotted against the left-hand axis) as a function of temperature, which for this measurement was increased at a rate of 10°C per minute. As the temperature increases, the mass decreases very slowly (due to an increase in vapour pressure as the temperature rises) until approximately 250°C, where the rate of mass loss rapidly increases with increasing temperature. This is reiterated by the first derivative of the mass (plotted against the right-hand axis), which illustrates the rate of mass loss which again is approximately zero until the temperature reaches ~250°C, upon which the rate of evaporation rapidly increases until it reaches a maximum at 372.5°C. Note however that the curve shown is actually the negative of the first derivative, which is accepted practice with the TGA technique and is plotted for convenience so that correlations between the two curves can be more easily observed.

When the TGA technique is used to determine boiling points of materials, standard practice is to extrapolate linearly along each of the two sections of the curve, both prior to evaporation and afterward, and take the temperature at their point of intersection, which for the Lumogen powder has been measured to be 328.6°C. Furthermore, the shape of the thermogram suggests that Lumogen powder as supplied by BASF is relatively pure (quoted purity is 99.9%), as there are no intermediate thermal events caused by loss of components or impurities such as water. The residue left in the pan (4.934%) is within standard experimental expectations. This residue, which was black in appearance, is quite probably carbon due to pyrolytic decomposition at some point before 400°C

Differential scanning calorimetry (DSC) was employed in order to further probe the thermophysical properties of Lumogen. In DSC, the heat flow from the sample is measured as a function of temperature. The measurement involved heating the sample at 10°C per minute to 330°C, where it was held isothermally for five minutes to remove the thermal history, before cooling at 10°C per minute, holding at 0°C for five minutes and finally heating again to 330°C.

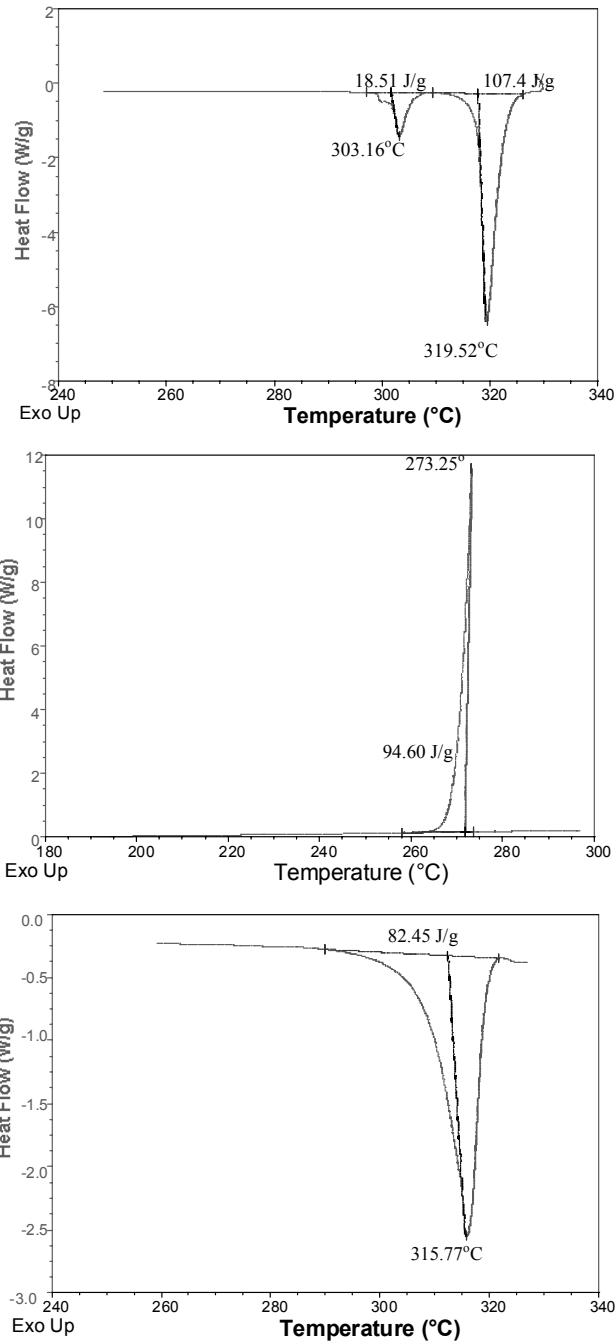


Figure 4. DSC thermograms of Lumogen powder showing (i) initial heating cycle (with 2 endothermic peaks); (ii) cooling cycle (with an exothermic peak) and (iii) the second heating cycle (with 1 endothermic peak). All temperature cycles were varied at a rate of 10°C per minute.

The initial heating cycle shown in figure 4 illustrates the temperature dependence of heat flow out of the sample for temperatures between 250°C and 330°C, with two negative valued peaks at 303.2°C and 319.5°C. These peaks indicate significant heat flowing into the sample (ie endothermic processes), as one would expect for a phase transition from solid to liquid, and thus each is indicative of a latent heat process that is associated with pure crystalline materials and suggests melting point values. It is possible that the existence of two peaks indicates two unique crystal phases that were initially present in the Lumogen powder, or that the material experiences a reconstruction (assuming no pyrolytic breakdown occurs) during the heating process. In contrast, the cooling cycle shows an exothermic peak that illustrates a phase transition in going from the liquid to solid state, and is observed to occur at 273.3 °C.

For a pure material, it is expected that the onset temperatures during the melting (temperature increasing) and recrystallisation (temperature decreasing) latent heat processes should occur at the same temperature value, ie the melting point of the sample. In the measurements reported here, the onset during heating occurs just above 295 °C, and during cooling recrystallisation occurs at approximately 275 °C. This appears to be consistent with an earlier report of the melting point of the material being 295°C [7].

The third plot in the figure shows a second heating cycle, and was performed in case the first heating cycle possessed some thermal history of the sample. In that case, the two endothermic peaks of the first cycle have been replaced by a single, broader peak at 315.8°C. It is possible that the sample's behaviour changed during the second heating cycle simply because the cooling rate between them was sufficiently slow for single crystal domains to form during the cooling cycle, whereas the manufacturing process may produce different crystalline forms. The difference in the heat of fusions indicated between the two heating cycles suggests mass loss has occurred (approximately 35% for this measurement). This is comparable to the TGA result seen earlier in figure 3, which indicates a similar mass loss when the powder is heated to 330°C at 10°C per minute. The extra mass loss indicated by the DSC results can be attributed to the mass loss that would occur during the isothermal period at 330°C.

3.2 Crystallinity

In order to further understand the nature of the crystalline forms that may be present in Lumogen samples, X-ray diffraction (XRD) measurements were undertaken. The technique relies on a fixed X-ray source, and as the sample rotates through a polar angle θ , the detector rotates at an angle 2θ so that the angle it makes with the sample surface normal is identical to that of the source. The diffraction technique relies on the planes within crystalline domains of the sample satisfying the Bragg condition, namely

$$n\lambda = 2d \sin \theta ,$$

where $n = 1, 2, 3, \dots$ is the diffraction order, λ is the X-ray wavelength and d is the crystal plane spacing.

The existence of crystalline domains within the sample cause peaks to be observed in the XRD spectrum, as amorphous materials have no periodic array of atoms within their structure and hence their XRD spectra look like a broad bremsstrahlung background across all angles. Since the diffraction order is predominately unity and the wavelength of the source is constant, then inspection of the Bragg condition reveals that small angles of θ correspond to large values of plane spacing, d , and vice versa.

The XRD technique was applied to the Lumogen powder and the spectrum obtained is shown in figure 5. The data in the figure clearly indicate that the powder is crystalline in its as-received state, with many peaks in the spectrum indicating both long and short-range order within the powder material. Investigations to determine the precise crystallographic nature of the powder remain ongoing in our laboratory.

Figure 6 shows an XRD spectrum of a Lumogen coating, that has been vapour deposited upon an unheated glass microscope slide (ie substrate was at room temperature). The two predominant peaks in the spectrum occur at 2θ values of 14.1° and 14.4°, representing crystalline d -spacings of 7.29Å and 7.14Å respectively. An amorphous halo is also present in the spectrum, and has been identified as the background due to the amorphous glass microscope slide used as a substrate.

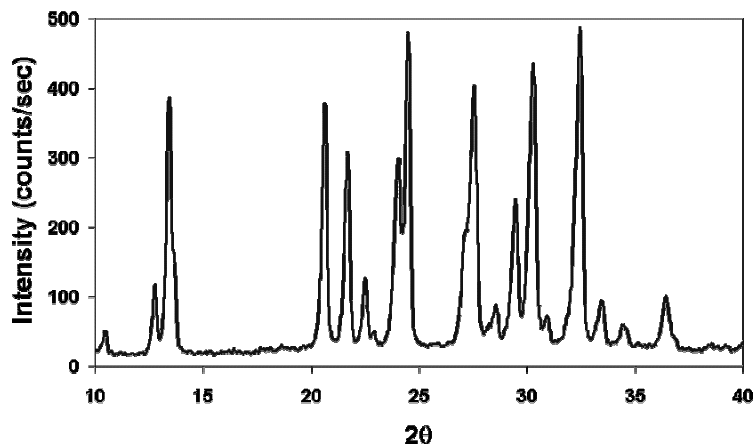


Figure 5. X-ray diffraction (XRD) spectrum of Lumogen Yellow S0790 in its 'as-received', powder state.

Other studies have shown that organic molecules may tend to exhibit planar geometries when adsorbed onto chemically inert surfaces [9]. The simplicity represented by the two lattice spacings observed for the as-deposited film suggests that this may indeed be the case with Lumogen. Moreover, the observed these lattice spacings are comparable to the estimated length of the Lumogen molecule, which is $\sim 7.4\text{\AA}$ along its longest axis.

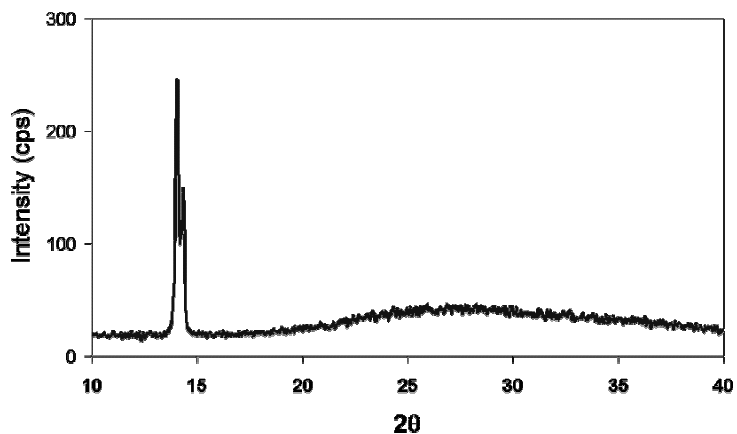


Figure 6. XRD spectrum of a Lumogen film deposited at room temperature upon a glass substrate (witness slide).

Some differences are observed between the XRD spectra of coatings deposited upon witness slides and those of bar samples positioned below the substrate heater, for the same coating run (even when the heater is not in use). The XRD spectrum of an as-deposited bar coating can be observed in figure 7. The two peaks at 2θ values of 14.1° and 14.4° can be observed, along with prominent peaks at 12.8° (7.96\AA), 13.5° (7.50\AA) and 27.7° (3.75\AA). The d -spacings of 7.50\AA and 3.75\AA seem indicative of the geometry of the Lumogen molecule. The presence of the broad amorphous background structure observed rising above the glass background for 2θ values between 20° to 40° are also noteworthy. In addition to this behaviour, bar samples were regularly observed to have peaks of lower intensities than their complementary witness slide. The precise reason for this is yet to be determined, however it is currently thought that the differences in the angle of incidence of adsorbing Lumogen molecules at the substrate may lead to directed preferential growth and thus sculptured films, which would lead to different diffraction characteristics.

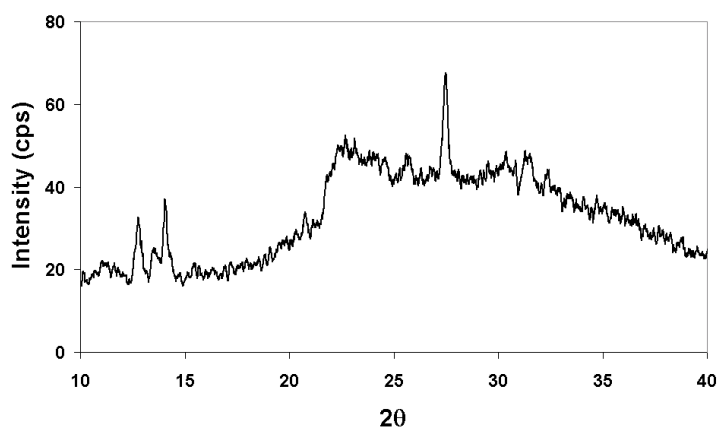


Figure 7. XRD spectrum of a Lumogen film deposited at room temperature upon a glass substrate (bar sample).

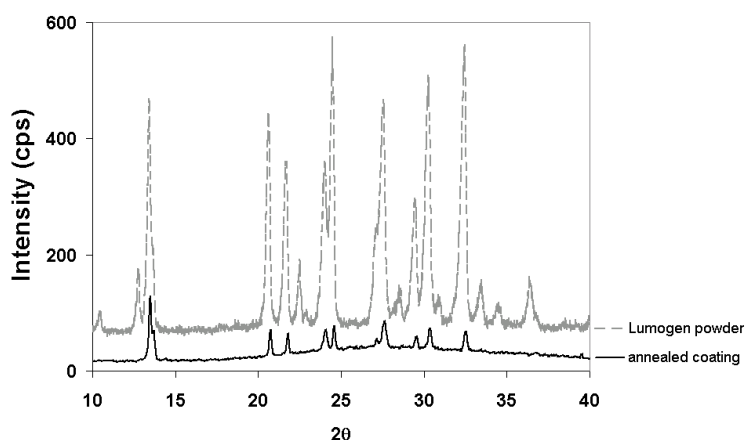


Figure 8. XRD spectra of (bottom trace) a coating annealed at 80°C and (top trace) Lumogen powder in its as-received state.

Part of our ongoing investigations into the crystal nature of these films is to study the influence of post-deposition storage upon crystal development. Figure 8 compares an XRD spectrum obtained from a room-temperature-deposited-coating after 90 hours of annealing at 80°C with the spectrum from the as-received powder. The peaks in the annealed coating spectrum appear to be in identical positions to the prominent peaks of the Lumogen powder spectrum. This result indicates that the crystal structure within the annealed coating is quite similar if not identical to the Lumogen powder. Moreover, this crystal structure is obviously different to that of the as-deposited coating as seen in figure 7, which is clearly observable through the loss of the amorphous background seen in the 2θ region between 20° and 40° of the as-deposited coating spectrum, and the subsequent growth of peaks in this same region seen for the annealing coating spectrum. The evolution of these peaks at relatively large values of 2θ , and thus relatively small d-spacing values, indicate a dramatic increase in short-range order within the film after annealing.

3.3 Surface Morphology

A scanning electron microscope (SEM) was used to examine Lumogen film surface morphology in each case. Figure 9 shows an SEM image of a control sample for the post-anneal study, in the form of an untreated room-deposited witness slide coating. The striking feature of the image is the textured appearance of the surface, which shows a microscopic non-uniformity upon coating. The image obtained from the witness slide coating can be compared to that obtained for a

similarly untreated bar sample produced during the same deposition, as presented in figure 10. In this image, the presence of numerous block-shaped mesoscopic crystals, which occupy larger domains than the features displayed in the background morphology, are clearly observable. These crystals exhibit a three dimensional nature, and their size is typically $\sim 0.5\text{-}2$ microns in length, is larger than the estimate thickness of the coating (600nm). It is also worthy of note that the level of texture in the background morphology appears to be less, and again may be due to sculpturing of the film.

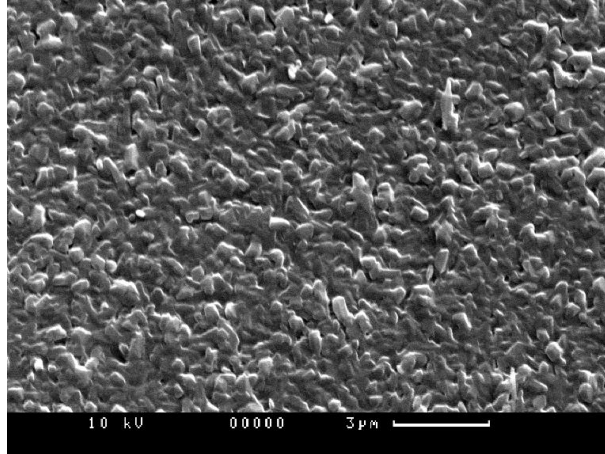


Figure 9. SEM image of an untreated room-deposited coating (witness slide).

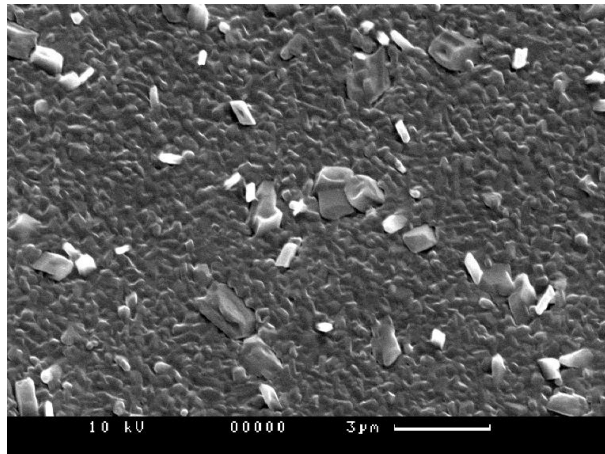


Figure 10. SEM image of an untreated room-deposited coating (bar sample).

A dramatic change in crystal morphology is observed, however, when the coatings are annealed. Figure 11 shows the SEM image obtained for a bar sample coating that was annealed for 90 hours annealing at 80°C . In this image, the crystals appear to have coalesced into a mat-like morphology. Furthermore, the size of the crystal domains have also appeared to increase, with typical structures of $\sim 1\text{-}5$ microns or larger in size. Within this morphology, a number of voids in the film can also be observed.

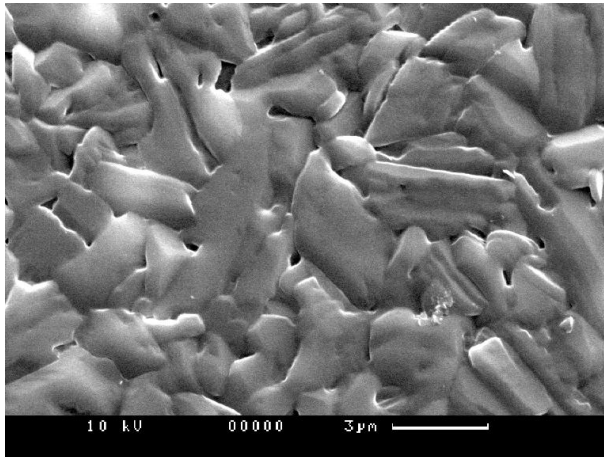


Figure 11. SEM image of a coating annealed at 80°C for 90 hours (bar sample)

3.4 Optical Characteristics

The absorption characteristics of Lumogen films were observed using ultraviolet-visible (UV-vis) spectroscopy. A UV-vis absorption spectrum obtained from a room-deposited Lumogen film upon a glass substrate is presented in figure 12. Absorption peaks associated with the electronic excitation characteristics of Lumogen are located at 335nm, 401nm, 425nm, and 456nm, and is in agreement with UV-vis data reported during early characterisation of Lumogen films by Kristianpoller [3]. The spectrum clearly demonstrates the ability of Lumogen Yellow S0790 to absorb radiation in the ultraviolet region of the spectrum, ie for wavelengths below 400nm. The absorption edge at 460nm lies below the emission band for Lumogen, which is known to occur over a range from 500nm to 650nm [3], thereby making it an ideal wavelength up-shifter.

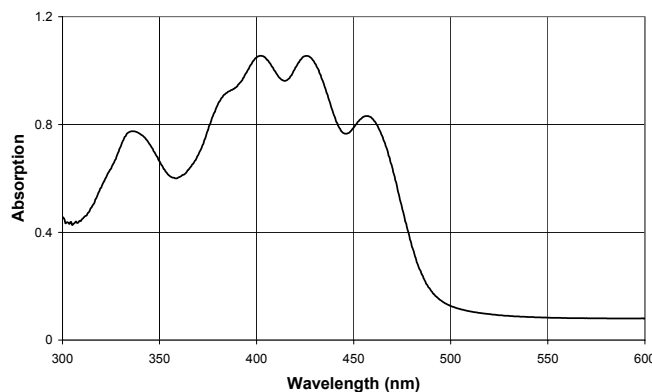


Figure 12. UV-vis absorption spectrum of an as-deposited coating deposited at room temperature.

The crystalline properties of various organic materials have previously been shown to influence that material's optical characteristics [10, 11] and hence this technique was used to perform preliminary investigations of the effect of crystallisation within the film upon its optical properties. However, this technique is limited to characterising very thin coatings, as the UV-vis instrument used actually operates by measuring transmittance and is limited to detecting 0.1% transmittance, which equates to films estimated to be < 200nm thick. Though not reported here, our preliminary results suggest that crystals developed through annealing cause significant variation in the UV-vis spectrum, but may be due to scattering effects of the film affecting the transmitted intensity. These investigations also continue in our laboratory.

4. SUMMARY

A number of measurements have been performed to characterise the nature of Lumogen powder and deposited optical films, with a view to investigating the crystallisation of Lumogen and with knowledge of this preparing tailored coatings for improved performance. Using thermogravimetric (TGA) analysis, Lumogen powder was found to have a boiling point of 328.6°C; and a melting point of approximately 295°C using differential scanning calorimetry (DSC).

Lumogen films prepared via a physical vapour deposition method were found to have an inherent crystalline structure in their as-deposited state, a structure and morphology that dramatically change upon annealing at 80°C, as evidenced by X-ray diffraction data and scanning electron microscopy imaging respectively.

Preliminary UV-vis results show these changes in the crystalline nature of the films affect its optical properties. It is expected that tailoring the structure within these films will enable the production of optical coatings with tailorable optical properties and thus improved performance.

REFERENCES

1. G. Naletto, E. Pace, G. Tondello and A. Boscolo, *Performance of a thinned back-illuminated ion-implanted CCD as detector for a normal incidence EUV spectrograph*. Measurement Science and Technology, **5**, 1491-1500, 1994.
2. P. F. Morrissey, S.R. McCandliss, and P.D. Feldman, *Vacuum-ultraviolet quantum efficiency of a thinned, backside-illuminated charge-coupled device*. Applied Optics, **34**(22), 4640-4650, 1995.
3. N. Kristianpoller, and D. Dutton, *Optical Properties of "Lumogen": A Phosphor for Wavelength Conversion*. Applied Optics, **3**(2), 287-290, 1964.
4. N. Kristianpoller and R.A. Knapp, *Some Optical Properties of Sodium Salicylate Films*. Applied Optics, **3**(8), 915-918, 1964.
5. M. M. Blouke, M. W. Cowens, J. E. Hall, J. A. Westphal and A. B. Christensen, *Ultraviolet downconverting phosphor for use with silicon CCD imagers*. Applied Optics, **19**(19), 3318-3321, 1980.
6. J. Perry, N. Mardesich, G. Frascchetti, T. Elliot, J. Janesick and S. Chung, *Report on Cassini ISS CCD Lumogen Film Problem*, Jet Propulsion Laboratory Internal Report, Pasadena, 1995.
7. J. Janesick, *Scientific Charge-Coupled Devices*, SPIE, Bellingham, Washington, 2001.
8. N. Mardesich, *Lumogen Deposition Procedure*, Jet Propulsion Laboratory, 1989.
9. G. Witte and C. Wöll, *Growth of aromatic molecules on solid substrates for applications in organic electronics*. Journal of Materials Research, **19**(7), 1889-1916, 2004.
10. G. Weiser and S. Möller, *Influence of molecular anisotropy on the optical properties of nanocrystalline films of π -conjugated systems*. Organic Electronics, **5**(1-3), 2004.
11. J. K. Politis, J.C. Nemes, and M.D. Curtis, *Synthesis and Characterization of Regiorandom and Regioregular Poly(3-octylfuran)*, Journal of the American Chemical Society, **123**(11), 2537-2547, 2001.